ADVANCED FUNCTIONAL MATERIALS
www.afm-journal.de

Multi-Stimuli Responsive Hydrogel Cilia

*P. J. Glazer, J. Leuven, H. An, S. G. Lemay, and E. Mendes**

Large arrays of high aspect ratio, artificial hydrogel based cilia that can respond to multiple stimuli are produced by means of micro-fabrication techniques. The cilia operate in aqueous solutions and are sensitive to pH, electric and/or magnetic fields. The biomimetic system combines both sensing and motility. Detection of changes in environment, such as a decrease in pH, triggers a collective response, to an external time-dependent magnetic field.

1. Introduction

There is significant demand for smart materials and sensors that can adapt and actuate in response to environmental or external stimuli. Research fields ranging from medicine to materials science and physics are interested in polymeric materials that are able to mimic artificial muscles, swell, shrink or bend in response to environmental stimuli. Among such materials, polyelectrolyte gels have attracted particular attention as they can exhibit discontinuous volume phase transitions triggered by small variations of external parameters such as temperature, electric field, solvent quality or pH.[1–4] We have recently shown that the characteristic response time of macroscopic polyelectrolyte gels to DC electric fields, while very sensitive to electrode/gel configuration, is in general governed by transport of ions and water across the gel.[5] Therefore, the actuation speed can be significantly improved by using systems with small dimensions. This fact already prompted the use of polyelectrolyte gels in miniaturized actuators such as stimuli-responsive valves[6] or active drug delivery systems.[7] However, despite the unique properties of polyelectrolyte gels, the fabrication of micrometer-scale responsive structures over large areas still remains a challenge.

In nature, many surfaces are covered with various sorts of fibrillar structures. This coverage with pillar-like geometry has some universal benefits. The functions of cilia in nature can be broadly divided into two categories: motile cilia that induce movement by constantly beating in a given direction[8] and stationary cilia that typically act as a chemical sensor to environmental changes.[9] However, some motile cilia in nature combine both functions and contain sensors to detect the change in external environment that triggers their movement.[10] Research on biomimetic cilia, based on microfabrication, has achieved significant advances in the last years.[11] The cilia-like geometry, which can fulfil diverse functions ranging from motility to chemical sensing of environmental changes, is a promising candidate for microfluidic, bio-mimic and lab-on-a-chip applications. The source of stimuli can vary and depends on the material used. A mechanical or chemical response is observed in response to environmental stimuli (pH,[12,13] chemical reaction–Belousov-Zhabotinsky reaction,[14] humidity,[15,16] light,[13,17]) or in response to electrical[11,18]/magnetic[19,20] signals. In the latter case, electrostatic or magnetic energy is directly converted into mechanical energy.

Toonder et al. fabricated electostatically actuated flap-like polymer structures that can generate fluid flow in microfluidic channels.[21] A similar idea was also proposed by Belardi et al.[22] The flap-like structures in the latter work, which were made from polymer gel and filled with magnetic particles, actuated in response to magnetic fields. Recently, Le Digabel et al. successfully incorporated magnetic particles inside polyacrylamide hydrogel micropillar structures.[19] However, the maximum displacement of those hydrogel structures in response to magnetic fields was on the order of few micrometers only. Evans et al. also fabricated nano-sized, highly responsive magnetic cilia made from PDMS prepolymer containg iron oxide nanoparticles that was poured into polycarbonate track-etched membrane which served as a mold.[20]

In this paper we present a large scale multi-responsive system that can be stimulated environmentally (pH), electrically (electrochemical reactions occurring on the electrodes) or magnetically (magnetic field). Making use of lithography techniques, we created high-aspect ratio molds on which the polymer solution was cast. The resulting structures are stable, highly responsive and their geometry is controlled. In case of environmentally or electrically stimulated actuation of the cilia, the size of each individual cilium can be reversibly reduced up to 89%. When a rotating magnetic field is applied to cilia filled with iron particles, the maximum cilium end displacement achieved is around 45-μm for 10-μm-thick and 55-μm-long cilium, and is only limited by the single cilium length. The results presented below combine, in a single system, magneto-responsiveness with sensing of environmental pH variations. As a result, microfabricated cilia move under a time-dependent magnetic field only when triggered by a pH change.

P. J. Glazer, J. Leuven, Dr. H. An, Dr. E. Mendes
Delft University of Technology
Chemical Engineering Department
Julianalaan 136, 2628 BL Delft, The Netherlands
E-mail: e.mendes@tudelft.nl
Prof. S. G. Lemay
University of Twente
MESA+ Institute for Nanotechnology
PO Box 217, 7500 Enschede, The Netherlands

DOI:10. 1002/adfm.201203212

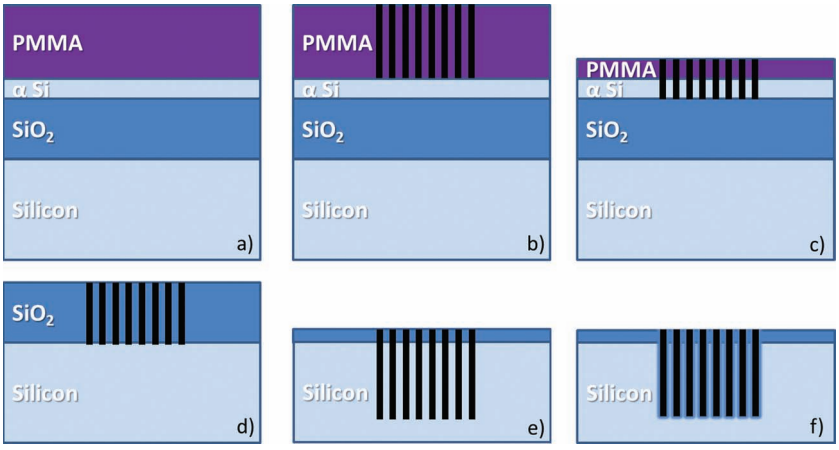

Figure 1. Process of high-aspect ratio silicon mold microfabrication: a PMMA layer is spin-coated on a silicon chip (a), and the cilia pattern is transferred on this layer by means of electron beam lithography (b). Subsequently three etching steps transfer the pattern deep into silicon (c–e). In the final step a thin layer of silicon dioxide is added by means of PECVD (f). A detailed description of the fabrication process is given in the text.

2. Results and Discussion

2.1. Mold Microfabrication

The basic fabrication steps of the high aspect ratio (a ratio of height to lateral feature size) silicon wafer mold are illustrated in **Figure 1**. First the silicon chip (1.9 cm × 1.9 cm) is cleaned by hard sonication in fuming nitric acid (Sigma Aldrich HNO_3> 90%), followed by thoroughly washing with demineralized and deionized water and isopropanol (IPA) and blowing dry with nitrogen. A 2-µm-thick layer of silicon dioxide, followed by 0.5-µm-thick layer of amorphous silicon, is then deposited on top by means of Plasma-Enhanced Chemical Vapour Deposition (PECVD, PlasmaLab 80 plus). Polymethylmethacrylate (PMMA,950 kDa–7% dissolved in Anisol) is then spin coated (Figure 1a) and the cilia design is transferred by means of electron beam lithography (EBPG 5000+ Leica) (Figure 1b). The exposure dose is set to 1000 µC/cm^2. For pattern developing, after e-beam exposure, a mixture of methyl isobutyl ketone (MIBK) and IPA is used (1:3 ratio). After developing, three Deep Reactive Ion Etching (DRIE) steps are performed in an Alcatel Microsystems AMS 100 system and each step has a different goal (Figure 1c–f). In the first DRIE step, the pattern is etched into the amorphous silicon with the PMMA layer serving as a mask (Figure 1c). The next step uses amorphous silicon as a mask and transfers the pattern into the silicon dioxide (Figure 1d). In the third DRIE step, silicon dioxide serves as a mask and the highly selective Bosch etching process is used to create vertical rectangular or cylindrical prisms deep into the silicon (Figure 1e). A general Bosch process cycle contains two phases: etching and passivation. In the etching step a mixture of fluorine based gasses etches the silicon and in the passivation step a polymer layer is deposited on the sidewall of the structure, which protects silicon sidewall from chemical erosion in the following etching step. This allows high-aspect-ratio feature generation.[23] In the last fabrication step, a thin oxide layer is added (~70 nm) by means of PECVD (Figure 1f). The overview of the microfabricated mold and its cross-section are illustrated in **Figure 2**. The highest aspect ratio achieved is around 50: cilia 1-µm thick and 50-µm long. It is important to stress that the size of the cilia arrays (around 6 mm^2) is only determined by the molding area and can easily be scaled up to full wafer scale.

2.2. Electro-Responsive Cilia

In order to form high-aspect-ratio gel cilia-like structures inside the microfabricated mold, with the mechanical properties that make the cilia suitable for electro/magnetoactuation, two main aspects need to be considered: (1) the cilia's mechanical properties, which are determined by the acrylamide/bis-acrylamide ratio, and (2) the precise mold filling, driven by capillary action, which is a function of polymer solution surface tension and adhesive forces between the polymer and the mold.

Because of the extremely high aspect ratio (up to 50) it is impossible to directly mold hydrogels from their monomers without additional silicon mold surface modification. To verify to what extent surface properties determine cilia development, we cast the monomer solution on the silicon mold surface which had been treated a priori either by plasma discharge (to make the substrate hydrophilic) or by silane vapors (which makes the mold surface hydrophobic). The results obtained are illustrated in **Figure 3**.

When the mold is hydrophilic, the monomer solution cannot fully access the mold due to its hydrophobic nature. As a consequence, the cilia are not developed as illustrated in Figure 3a. On the contrary, when the silane layer is added the adhesive forces promote complete mold filling and the cilia are fully

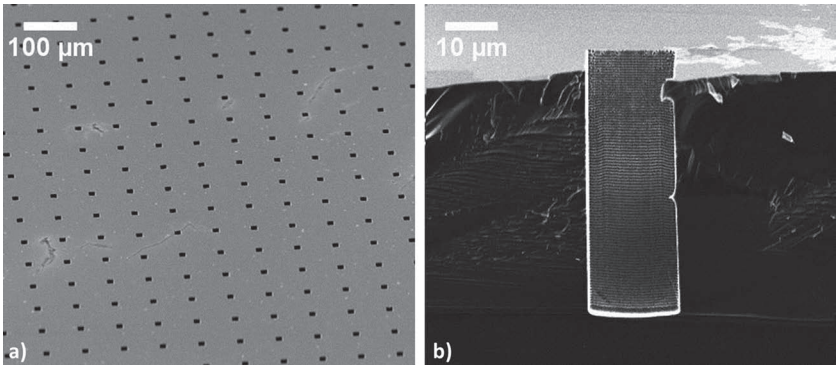

Figure 2. Scanning electron microscope images of a typical microfabricated silicon mold: a) general mold overview (top view) and b) cross section obtained after cleaving the wafer.

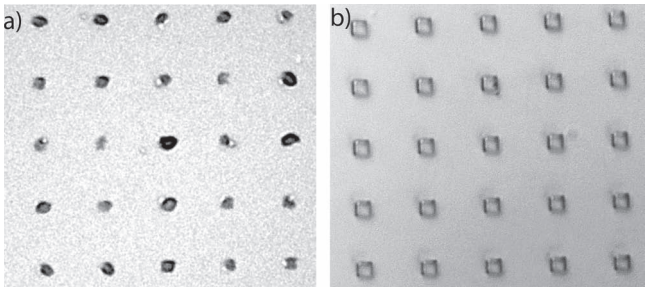

Figure 3. Cilia development after casting polymer solution on a) a hydrophilic (plasma treated) mold and b) a hydrophobic (silanized) mold (cilia immersed in aqueous solution).

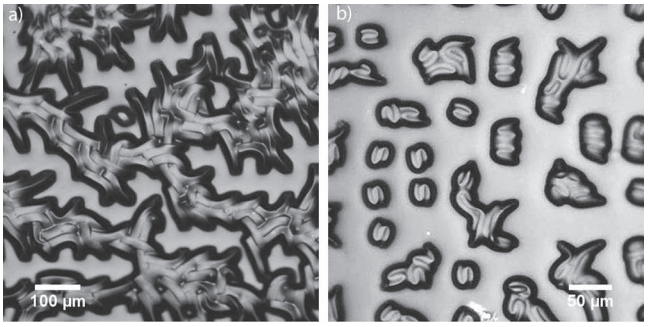

Figure 4. Polyacrylamide gel cilia (in air) developed on a silanized silicon mold. The single cilium thickness is 15 µm for (a) and 2 µm for (b).

developed and long (see Figure 3b and **Figure 4**). Figure 3 therefore indicates that, to a large extent, mold surface properties determine the cilia development.

Polyacrylamide gel cilia released from the mold are extremely flexible. This is illustrated in Figure 4. The cilium can twist its structure two times under an angle of 90 degrees without any visual structural defects (Figure 4b). When in air, the longest (up to 100 µm) cilia collapse or entangle because the elastic strain energy of the gel matrix is smaller than the adhesive forces between the cilia[24] (more images in the Supporting Information). When the pillars are immersed in water they immediately disentangle and all point up as already shown in Figure 3b. The speed at which this process occurs is displayed in Supporting Information Video 1.

To make the released polyacrylamide cilia electro-responsive, the gel is placed in a 2 M NaOH solution (Sigma Aldrich, 71689, purity > 98.0%) to hydrolyse the amine groups R-NH_2. This process is limited by diffusion, so the time needed for complete hydrolysis varies with the gel size. In the present work a period of 2 days is used.

When the gel is placed in a 2 M NaOH solution, the amine groups are converted into ionized carboxylic groups. The maximum efficiency of the groups conversion is about 20%.[1,25] Charges on the gel network are set by the $–COO^-$ groups and are neutralized by Na^+ counter ions. The gel is then placed in an excess of demineralised and deionised water, and the osmotic pressure difference induces gel swelling. As the gel volume increases, the density of ionized groups decreases, therefore also reducing the osmotic pressure difference. Each time the water is replaced, the gel reaches a new final volume as a balance between polymer matrix-solvent affinity and network elasticity, which resists expansion.[26] Swollen cilia capable of electro-actuation are illustrated in Supporting Information Figure S3.

The electro-responsiveness is tested by means of two platinum wire electrodes attached to micromanipulators mounted on the microscope table (see the Supporting Information for detailed description of the experimental setup). As illustrated in **Figure 5**, an actuation wave propagates from the anodic electrode a short moment after a voltage difference (3 V) is applied with each individual cilium shrinking when the actuation front reaches it (the electrode and associated gas evolution are visible as a dark region on the left of the image). Approximately 20 s after the initial actuation, the complete array has shrunk. The shrinkage of an individual cilium is depicted in Figure 5b (see also the Supporting Information Video 2). The contracted cilia expand again when the polarity of the electrodes is reversed. During the course of the experiments, no visual mechanical defects of the cilia were observed while changing the electrodes polarity.

Based on the above observations, it is plausible that, in this case where the gel cilia are in the vicinity of the electrodes, the electrochemical reactions occurring at the electrodes drive electro-actuation. In particular, when an electric potential above 1.2 V is applied across Pt electrodes immersed in aqueous solutions, hydronium and hydroxide ions are created at the electrode surfaces by water electrolysis.[27] These ions are then transported away from the electrodes and into solution under the influence of diffusion and the applied electric field. That is, a pH wave originates from each electrode and propagates with a velocity that is a function of applied voltage.[5] These changes in local pH in the anode vicinity (low pH) can cause the chemical equilibrium of the carboxylic groups inside the gel to shift,

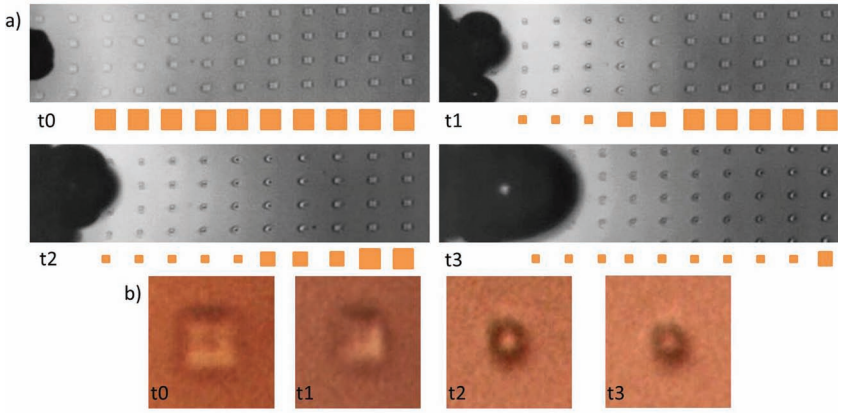

Figure 5. a) Key-frames of the actuation wave propagating along the array when the voltage difference is applied. The spatial progression of the shrinking process is further illustrated by the size of the orange squares below each image; b) Shrinkage of the single cilium cross-section. The labels t0–t3 indicate time evolution.

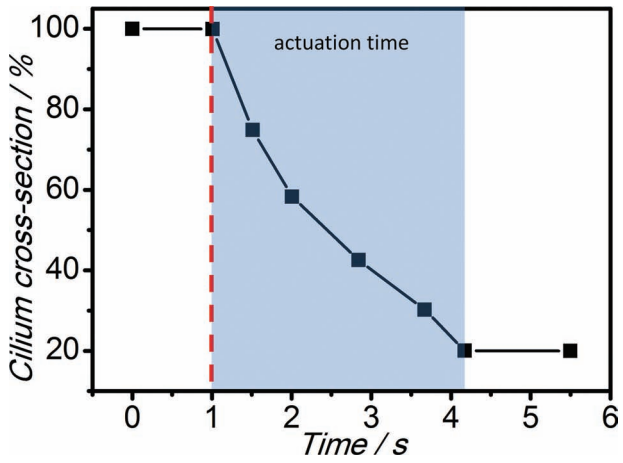

Figure 6. Cilium cross-section vs. time. At time t = 1 s (marked with red line) the pH wave reaches the cilium (the line is added to guide the eye).

which can in turn result in cilia shrinkage. When the polarity of the electrodes is reversed, the opposite process can increase the local pH value and ionize the gel again, which induces water uptake to balance the electrostatic repulsion between ionized groups attached to the polymer backbone.

To demonstrate whether the cilia electro-actuation and the pH wave caused by water electrolysis are associated phenomena under the present conditions, an experiment with actuating cilia in the presence of a pH probe is conducted. This enables the visualization of the pH wave coming from the electrode (see the Supporting Information Video 3) and allows comparing its time evolution with the actuation wave. The moment from the first noticeable shrinkage or swelling until the stabilization of the cilium size is defined as the actuation time. **Figure 6** shows the result of an actuation experiment, in the presence of pH indicator, in which the change in area of a single cilium is observed. The visible actuation starts when the pH front reaches the cilium and a significant area reduction is reached within 3 s after the pH front passes the observed cilium. This area reduction is approximately 80%, as obtained from the digital images similar to Figure 5b.

To further validate that local pH variations are responsible for cilia actuation, we conducted an experiment in which a drop of low pH solution is added directly above the array during observation. As shown in **Figure 7**, at the moment that the pH is locally lowered, significant cilium area reduction occurs. This confirms that the cilia shrinkage is a pH driven process. For pH 1 solution, the observed 89% area reduction is 12% greater than when electro-activated. For pH 3 solution, the area reduction is at least 80% but cannot be determined very accurately due to a rapid recovery toward the initial size after approximately 2 s.

It is important to stress that the electrode vicinity implies the actuation mechanism described above. In case of macroscopic samples and electrodes placed further apart, different or additional mechanisms are triggering electro-actuation of hydrolysed polyacrylamide gels.[2,3,5]

2.3. Magneto-Responsive Cilia

In the previous part, stationary cilia which can act as a chemical sensor to environmental changes were introduced. We now focus on motile cilia that can move in response to external magnetic field stimuli. The cilia synthesis scheme is the same; however, in order to obtain magneto-responsiveness, we selectively place magnetic iron particles inside the cilia. To achieve this goal, the gel mold, located inside a plastic container filled with 1 µm iron particles (BASF), is placed on a laboratory shaker for 15 min. Due to the lateral movement of the shaker in conjunction with gravity, the particles fill in the mold. The mold is then removed from the container and its surface is carefully cleaned with adhesive tape. In order to avoid the particles leaving the mold pits during gelation, a permanent magnet is placed beneath the mold. The monomer solution is then cast on the silicon mold, followed by addition of APS and TEMED, and left overnight to complete polymerization. It is important to stress that the adhesive tape-cleaning procedure slightly depletes the base of the cilia from iron particles, which creates additional cilia flexibility.

The magneto-responsiveness is tested by means of a self-built setup generating a rotating magnetic field in the horizontal plane, mounted on a Nikon Eclipse microscope (see the Supporting Information for detailed description of the experimental setup). **Figure 8** shows synchronized movement of 10-µm-thick and 55-µm-long cilia imposed by the rotating magnetic field, leading to an average deflection of around 40 µm. Even at a high magnetic field frequency (cilia rotating at more than 160 rpm) the movement is unperturbed and no visual defects after thousand cycles are visible (see the Supporting Information Videos 4 and 5).

From Figure 8 (and the Supporting Information Videos 4 and 5), it can be observed that large arrays of cilia that could be collectively actuated by magnetic field were fabricated. The cilia rotation speed can easily be adjusted by changing the magnetic field rotation frequency. In addition, directional movement of the cilia towards the source of the magnetic field is

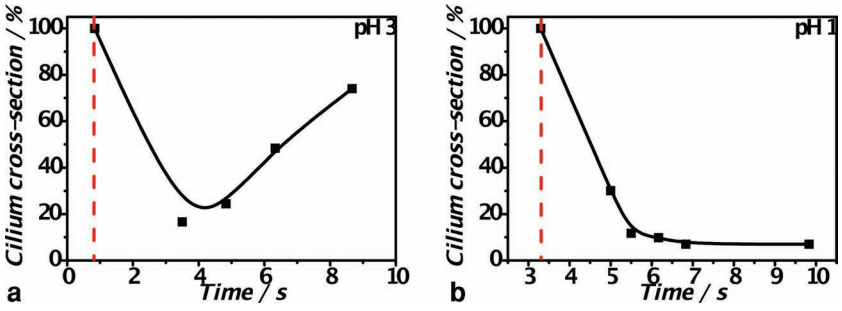

Figure 7. Cilium cross-section as a function of time. At the time marked with the red line, 20 µL of a) pH 3 and b) pH 1 solution were added directly above the observed cilia (the lines are guides to the eye).

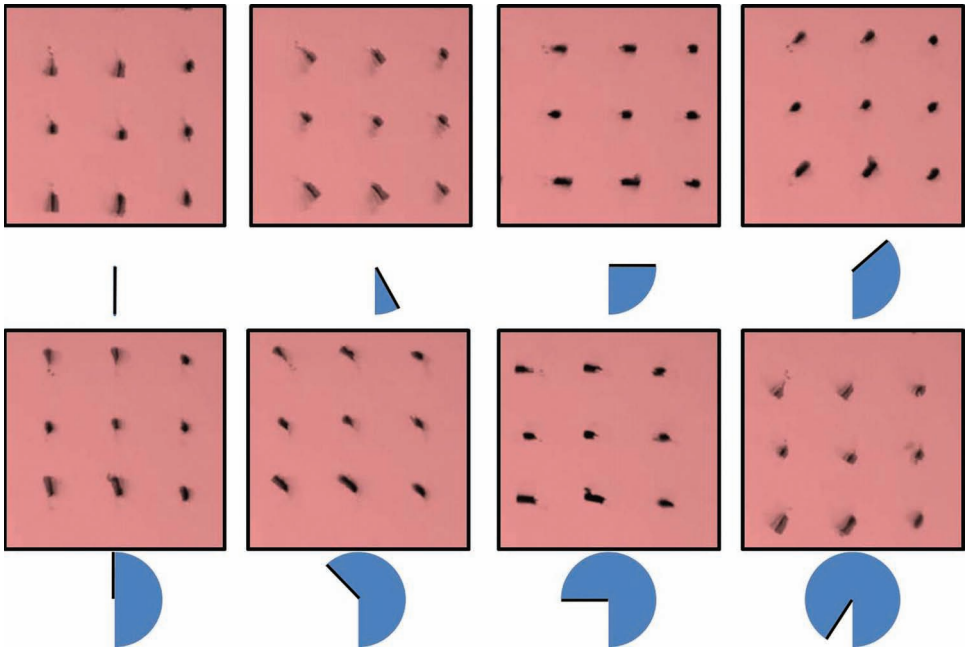

Figure 8. Cilia rotation in response to an external rotating magnetic field. Total time: 2 s.

achieved when applying the field with a permanent magnet. Such a magnetically-tuneable array could be implemented in bio-mimicking systems, in which collective transport over large areas still remains a challenge.

With the help of ImageJ software, we mapped the single cilium tip position over 10 rotating cycles (see the Supporting Information Video 6). This analysis shows that the cilium displacement follows the magnetic field direction in a reproducible way (**Figure 9**).

2.4. Multi-Responsive Cilia

In the previous parts we have introduced two versatile systems that can be externally activated, namely, non-motile cilia activated electrochemically or by local pH change, and motile cilia which respond to a magnetic field. In the following part we present a combined multi-stimuli system that initiates rotational motion when the local pH is lowered. The magnetic cilia prepared as described above are first hydrolysed and swollen in ionized and demineralized water. The magnetic particles are embedded in the gel matrix and redistribute while the gel swells. It is important to stress that even significant swelling does not damage individual cilia. This procedure combines magneto- and electro- responsiveness in a single system. The cilia are then placed in a rotating magnetic field. In the swollen state, no visual response is observed. However, when the local pH is lowered, with the droplet of pH 1 solution, cilia start to shrink and rotate. **Figure 10** illustrates the actuation and the intermediate phases when the pH is lowered. In the shrunken state the cilium is bent at the base under an angle that is determined by the magnetic field's orientation and follows the field rotation (see the Supporting Information Video 7 for more details).

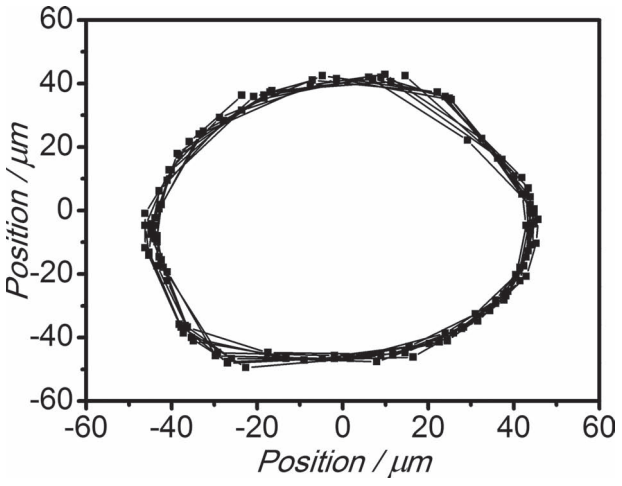

Figure 9. Cilium tip position within 10 full cycles.

3. Conclusions

We have fabricated large high-aspect-ratio responsive cilia arrays that combine, in one system, sensing and motility functions. Based on different approaches the system can be electrically, environmentally or magnetically activated. The fast response time and significant difference in size reduction between different pH values, which can easily be measured with optical methods, make this system a possible candidate for local pH-sensitive detectors and actuators. The combination of electro- and magneto-response in a single system further creates opportunities for creating new artificial bio-mimicking applications. To the best of our knowledge this is the first microfabricated cilia

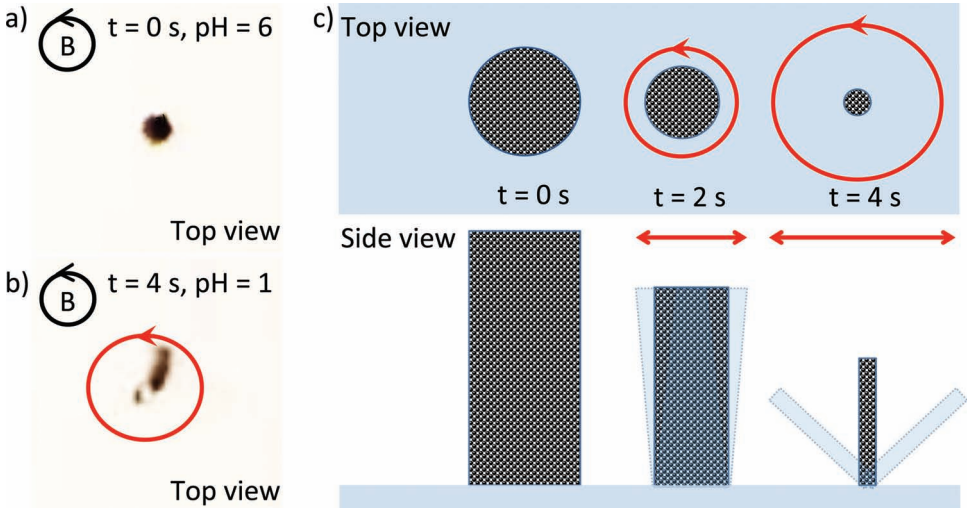

Figure 10. Hydrolyzed and swollen polyacrylamide cilia, filled with iron particles, do not respond to a rotating magnetic field when immersed in pH 6 solution (a). However, when the pH of the surrounding solution is lowered, by an addition of a pH 1 solution droplet, the individual cilia shrink and start to follow the magnetic field rotation (b). c) Schematic illustration of the magneto/pH responsive system, including intermediate phases.

system based on hydrogel that can respond to multiple stimuli (electric field, pH and magnetic field) simultaneously.

4. Experimental Section

Polyacrylamide gel synthesis is performed by free radical polymerization as described elsewhere.[5] First, 2.5 g of acrylamide solution (GERBU Biotechnik, acrylamide 40% solution; #1138,1000) and 1.5 g of methylene-bis-acrylamide aqueous solution (GERBU Biotechnik, bisacrylamide 2% solution; #1110,1000) are mixed with 16 g of demineralized and deionised water (MilliQ, resistivity higher than 18 MΩ cm). The acrylamide/bis-acrylamide ratio determines the gel stiffness. If the concentration of bis-acrylamide is too high, the structure becomes brittle, which renders gel handling very difficult. In addition, apart from actuation, cracks in the gel structure immediately appear when an electric field is applied. The acrylamide/bis-acrylamide ratio used yields a gel with good mechanical properties, suitable for both magneto- and electro-actuation, and was optimized by means of rheology measurements (see the Supporting Information for more details). To improve cilia development we add 1 wt% of sodium dodecyl sulfate (SDS, Sigma Aldrich, 436143, purity > 99%), which acts as a surface active agent and lowers the polymer mixture surface tension (see the Supporting Information). To facilitate filling of the high-aspect-ratio mold, we place the mold in the vapours of (tridecafluoro-1,1,2,2-tetrahydrooctyl)trichlorosilane (AB111444, ABCR). Directly before casting the monomer mixture, ammonium persulfate (APS, Sigma Aldrich, A3678, purity > 98%) is added (1/100 of total volume, 10% APS solution) as a radical initiator and *N,N,N′,N′*-tetra methylethylenediamine, (TEMED, Sigma Aldrich, T9281, purity > 99.0%) as an accelerator (1/1000 total volume). The solution is then immediately cast on the silicon mold and left overnight to complete polymerization, yielding a polyacrylamide gel.

To non-invasively visualize the dynamics of the pH gradient in situ during actuation, the gel sample is soaked in a universal pH indicator (Fluka #31282 - Universal indicator solution pH 3.0–10.0; 1:20 volume ratio of pH indicator and 0.1 M KCl solution).

Supporting Information

Supporting Information is available from the Wiley Online Library or from the author.

Acknowledgements

Serge G. Lemay acknowledges financial support from the European Research Council (ERC).

Received: November 1, 2012
Revised: December 7, 2012
Published online: January 18, 2013

[1] T. Tanaka, I. Nishio, S. T. Sun, S. Uenonishio, *Science* **1982**, *218*, 467–469.
[2] T. Shiga, T. Kurauchi, *J. Appl. Polym. Sci.* **1990**, *39*, 2305–2320.
[3] M. Doi, M. Matsumoto, Y. Hirose, *Macromolecules* **1992**, *25*, 5504–5511.
[4] Z. B. Hu, Y. Y. Chen, C. J. Wang, Y. D. Zheng, Y. Li, *Nature* **1998**, *393*, 149–152.
[5] P. J. Glazer, M. van Erp, A. Embrechts, S. G. Lemay, E. Mendes, *Soft Matter* **2012**, *8*, 4421–4426.
[6] D. J. Beebe, J. S. Moore, J. M. Bauer, Q. Yu, R. H. Liu, C. Devadoss, B. H. Jo, *Nature* **2000**, *404*, 588–590.
[7] P. Bawa, V. Pillay, Y. E. Choonara, L. C. du Toit, *Biomed. Mater.* **2009**, *4*, 022001.
[8] N. Hirokawa, Y. Tanaka, Y. Okada, S. Takeda, *Cell* **2006**, *125*, 33–45.
[9] V. Singla, J. F. Reiter, *Science* **2006**, *313*, 629–633.
[10] A. S. Shah, Y. Ben-Shahar, T. O. Moninger, J. N. Kline, M. J. Welsh, *Science* **2009**, *325*, 1131–1134.
[11] Z. G. Zhou, Z. W. Liu, *J. Bionic Eng.* **2008**, *5*, 358–365.
[12] L. D. Zarzar, P. Kim, J. Aizenberg, *Adv. Mater.* **2011**, *23*, 1442–1446.
[13] F. Liu, D. Ramachandran, M. W. Urban, *Adv. Funct. Mater.* **2010**, *20*, 3163–3167.
[14] O. Tabata, H. Hirasawa, S. Aoki, R. Yoshida, E. Kokufuta, *Sens. Actuators, A* **2002**, *95*, 234–238.
[15] D. Chandra, J. A. Taylor, S. Yang, *Soft Matter* **2008**, *4*, 979–984.
[16] A. Sidorenko, T. Krupenkin, A. Taylor, P. Fratzl, J. Aizenberg, *Science* **2007**, *315*, 487–490.
[17] T. Watanabe, M. Akiyama, K. Totani, S. M. Kuebler, F. Stellacci, W. Wenseleers, K. Braun, S. R. Marder, J. W. Perry, *Adv. Funct. Mater.* **2002**, *12*, 611–614.

[18] E. W. H. Jager, E. Smela, O. Inganas, *Science* **2000**, *290*, 1540–1545.
[19] J. le Digabel, N. Biais, J. Fresnais, J. F. Berret, P. Hersen, B. Ladoux, *Lab Chip* **2011**, *11*, 2630–2636.
[20] B. A. Evans, A. R. Shields, R. L. Carroll, S. Washburn, M. R. Falvo, R. Superfine, *Nano Lett.* **2007**, *7*, 1428–1434.
[21] J. den Toonder, F. Bos, D. Broer, L. Filippini, M. Gillies, J. de Goede, T. Mol, M. Reijme, W. Talen, H. Wilderbeek, V. Khatavkar, P. Anderson, *Lab Chip* **2008**, *8*, 533–541.
[22] J. Belardi, N. Schorr, O. Prucker, J. Ruehe, *Adv. Funct. Mater.* **2011**, *21*, 3314–3320.
[23] S. Franssila, J. Kiihamaki, J. Karttunen, *Microsyst. Technol.* **2000**, *6*, 141–144.
[24] Y. Zhang, C. W. Lo, J. A. Taylor, S. Yang, *Langmuir* **2006**, *22*, 8595–8601.
[25] W. M. Leung, D. E. Axelson, D. Syme, *Colloid Polym. Sci.* **1985**, *263*, 812–817.
[26] P. Flory, *Principles of Polymer Chemistry*, Cornell University Press: Ithaca, New York **1953**.
[27] H. B. Schreyer, N. Gebhart, K. J. Kim, M. Shahinpoor, *Biomacromolecules* **2000**, *1*, 642–647.